2025 IEEE Topical Conference on Wireless Sensors and Sensor Networks (WiSNeT) | 979-8-3315-0733-6/25/$31.00 ©2025 IEEE | DOI: 10.1109/WiSNeT63956.2025.10905027

K-Band QPSK PMCW Radar with Digital *I/Q* Constellation Phase Compensation and *I/Q* Imbalance Correction

Derek Thompson
Dept. of Electrical and Computer Engineering
Texas Tech University
Lubbock, TX, USA
derek.thompson@ttu.edu

Changzhi Li
Dept. of Electrical and Computer Engineering
Texas Tech University
Lubbock, TX, USA
changzhi.li@ttu.edu

***Abstract*—This paper presents a novel *K*-Band Quadrature Phase Shift Keying (QPSK) phase-modulated continuous-wave (PMCW) radar front end architecture with digital *I/Q* constellation phase compensation and *I/Q* channel imbalance correction. Although QPSK is a very common form of digital phase modulation, it is rarely reported for PMCW radar systems, especially those designed on printed circuit board (PCB) technology. A MATLAB simulation platform is also developed and presented to help verify the benefits of QPSK PMCW radar for range detection.**

Keywords— I/Q channel imbalance, PMCW, phase modulation, QPSK, radar

I. Introduction

Phase-modulated continuous-wave (PMCW) radar is a type of radar sensor applicable to many wireless sensing environments [1]. With improving semiconductor technology, PMCW radar is becoming a more viable solution for modern sensor architectures. Although this paper does not explore automotive applications, Fig 1. shows a scenario where automotive application of PMCW radar may help to mitigate interference due to its single-frequency carrier and the adaptability of its encoding waveform [1]-[4]. The single spread carrier of PMCW creates a broad increase in system noise floor [1], [4] but opens potential channels for more efficient use of decreasing electromagnetic spectrum resources [5]. Typical PMCW radar systems leverage a phase modulation scheme known as binary phase shift keying (BPSK), where the carrier frequency is modulated with one of two different phases to encode digital sequences [9]. However, higher order phase modulation schemes such as quadrature phase shift keying (QPSK), where the transmitted signal is modulated with one of four different phases [10], are rarely explored for PMCW radar applications. To analyze the benefits of higher order modulation and improve the performance of PMCW radar systems, this paper presents a printed circuit board (PCB) technology QPSK PMCW radar operating in the *K*-band with digital *I/Q* constellation phase compensation and *I/Q* channel imbalance correction. A MATLAB simulation is also presented to overcome limitations in the high frequency bit stream encoding and sampling rates required for PMCW radar range detection and verify the advantages of QPSK for future PMCW radar sensors .

The authors wish to acknowledge the National Science Foundation (NSF) for funding support under Grant ECCS-2030094.

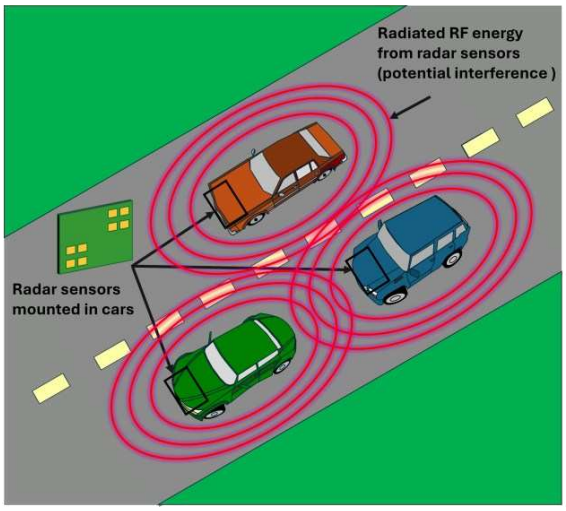

Fig. 1. Example automotive radar application where the waveform adaptability and single spread carrier of PMCW may improve interference mitigation.

II. PMCW Radar Theory and Simulation

A. PMCW Radar Theory

PMCW radar is a digitally modulated radar that uses phase modulation to encode digital information in the form of a pseudo-random binary sequences (PRBS) [7], [8]. The transmitted signal model of a PMCW radar can be represented by (1), where $X(t)$ represents the transmitted electromagnetic signal, f_c represents the carrier frequency, and $\phi_i(t)$ represents some random oscillator phase noise. The $\phi_m(t)$ represents the desired phase modulation term. For ideal BPSK modulation, $\phi_m(t)$ would be 0° or 180°. For ideal QPSK modulation the $\phi_m(t)$ term would be 0°, 90°, 180° or 270°.

$$X(t) = cos(2\pi f_c t + \phi_i(t) + \phi_m(t)) \quad (1)$$

The local oscillator (LO) signal is the same as (1) except without the extra $\phi_m(t)$ term. After mixing the reflected RF signal with the LO, it can be seen that the baseband signal from a PMCW radar leveraging *I/Q* demodulation is almost identical to the baseband *I/Q* signal of a continuous wave (CW) Doppler radar introduced in [11]. The mathematical model for the complex baseband signal is given by (2), where $\psi(t)$ is the total phase term that accounts for phase modulation, target distance, target motion and random phase error. The expanded form of $\psi(t)$ is represented by (3), where d_0 represents the distance to

the target, λ is the free space wavelength of the carrier signal and $x(t)$ is the target motion relative to the radar sensor. Furthermore, the expanded form of $\Delta\phi_i(t)$ and $\Delta\phi_m(t)$ are represented in (4) and signify the initial phase noise of the oscillator and desired phase modulation term that have been time shifted due to the round trip time delay of the electromagnetic wave.

$$B(t) = cos(\psi(t)) + jsin(\psi(t)) \tag{2}$$

$$\psi(t) = \frac{4\pi(d_0 + x(t))}{\lambda} + \Delta\phi_i(t) + \Delta\phi_m(t) \tag{3}$$

$$\begin{aligned} \Delta\phi_i(t) &= \phi_i\left(t - \frac{2d_0}{c}\right) \\ \Delta\phi_m(t) &= \phi_m\left(t - \frac{2d_0}{c}\right) \end{aligned} \tag{4}$$

The phase terms in the argument of the cosine and sine functions can ultimately add together to make a single resulting phase and therefore output voltage signal. In the case of a stationary target, the resulting output signal will be a constant DC voltage relative to the $\phi_m(t)$ term. The output level of the signal will change depending on the value of the $\phi_m(t)$ term, so the voltage is constant for the symbol period denoted by T_s. A symbol can be understood as a phase state that encodes one or more bits of digital information. In the case of a moving target, the baseband signal will be the superposition of the DC voltage level relative to the phase modulation term and the Doppler phase term relative to the target motion.

PMCW radar can detect range through its characteristic phase modulation. The demodulated *I/Q* baseband signal can be used to reconstruct a time-shifted version of the original PRBS. Then, autocorrelation of the reconstructed sequence and the original phase sequence returns a high correlation peak corresponding to the number of symbols the sequence is delayed. Therefore, the range resolution of PMCW radar is directly related to symbol frequency [1], [6]. The range resolution of PMCW radar is given by (4). Where ΔR is the range resolution in meters, T_s is the symbol period, f_s is the symbol rate and c is the speed of the light in meters per second which can be used as an accurate approximation for the speed of the electromagnetic wave.

$$\Delta R = \frac{cT_s}{2} = \frac{c}{2f_s} \tag{5}$$

To achieve high range resolution values, it is necessary to have a very high symbol rate [1]. However, with a known number of samples per symbol, the range resolution and target range bin can also easily be determined with proper down sampling of the received signal even at a lower symbol frequency. The burden of high sampling rates to achieve high range resolution has hindered the wider application of PMCW radar as opposed to the more common frequency modulated continuous wave (FMCW) radar [1]. With modern advancements in supporting hardware such as high-speed analog to digital converters (ADCs) and field programmable gate arrays (FPGAs) PMCW radar has become more accessible for modern wireless sensing applications.

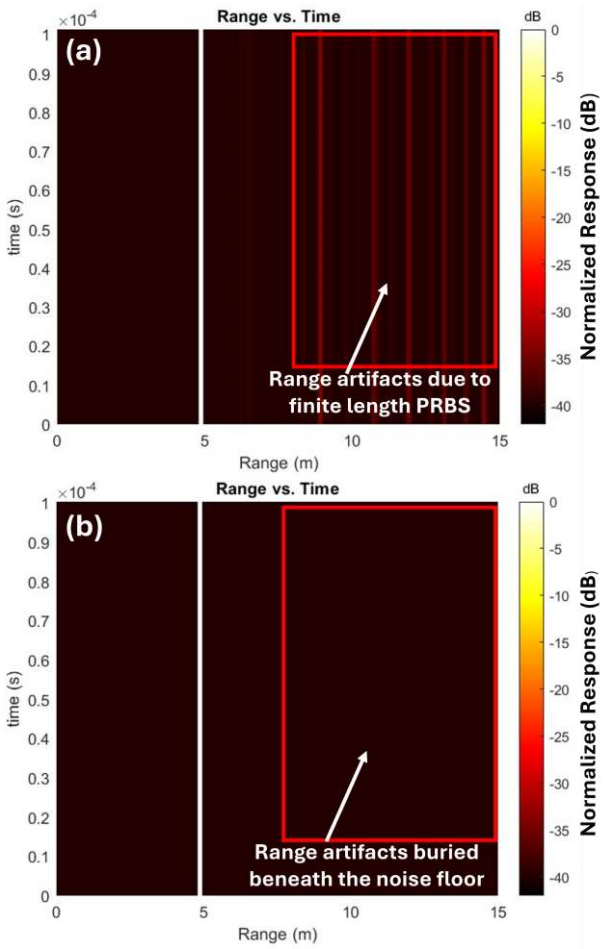

Fig. 2. PMCW radar range vs. time plots for (a) BPSK and (b) QPSK modulation for a single stationary target at 5 m with a 100 μs time window.

B. Simulation Study

A MATLAB simulation platform was developed using the well-known PMCW radar signal model to analyze the benefits of higher order QPSK modulation for modern radar sensors. The simulation helps to overcome the hardware limitations that limit the experimental results of this paper. The closed form expression for the baseband signal used for simulation is given by $f(t,n)$ in (6) and (7) where (6) is the baseband signal for the n^{th} symbol in a single PRBS and (7) gives the i^{th} sequence of $f(t,n)$. $\phi_m(n)$ denotes the phase shift of the n^{th} QPSK symbol, τ is the time delay due to the propagation of the electromagnetic wave and N_s is the total number of PRBSs.

$$f(t,n) \propto e^{j2\pi f_c(t)\tau + \phi_m(n)} \tag{6}$$

$$f_{BB}(t,n) = \sum_{i=1}^{N_s} f(t,n) \tag{7}$$

The above signal models give a platform for accurate mathematical modeling and analysis of the merits of QPSK for next generation PMCW radar.

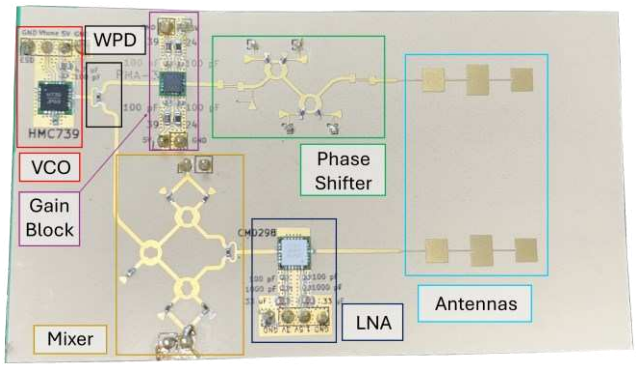

Fig. 3. K-Band QPSK PMCW Radar front end on Rogers R03003 substrate.

After applying a PMCW *I/Q* constellation phase compensation algorithm, the corrected data is reconstructed into a bitstream for autocorrelation with the original PRBS. Applying these steps to N_s total PRBSs, a range vs. time plot as shown in Fig. 2 can be constructed from the radar data.

The benefits of QPSK modulation can be visualized in the range time plots given in Fig. 2 (a) and Fig. 2 (b), which correspond to BPSK PMCW and QPSK PMCW, respectively, when analyzed in the same time window. In BPSK, each symbol encodes a single bit of digital information [9]. However, in QPSK, two bits are encoded per symbol [10]. Therefore, QPSK can achieve the same correlation values and SNR as BPSK in half the time window. Effectively, this doubles the range processing speed while retaining the same symbol rate. Similarly, SNR can be increased using QPSK. Fig. 2 demonstrates the SNR increase of an ideal QPSK PMCW radar when compared with its BPSK counterpart. In the same time window, QPSK can encode twice the amount of digital information. This leads to higher correlation values and results in a 3dB SNR increase in the received range spectrum. These results are clearly visible in Fig. 2 (b) where range artifacts due to finite length PRBSs in the range vs. time plot given in Fig. 2 (a) disappear. It is important to note that QPSK cannot double range processing speed and increase SNR at the same time. The respective benefit must be chosen for the applicable scenario.

III. *K*-Band QPSK PMCW Radar

A. Radar Sensor Hardware and Design

For experimental validation of the concepts introduced in Section II, a *K*-Band QPSK PMCW radar was fabricated on Rogers 3003 substrate. Fig. 3 shows the PMCW radar sensor front end. The carrier frequency of the sensor is 24 GHz. The architecture contains RF building blocks such as a voltage-controlled oscillator (VCO), low-noise amplifier (LNA), and gain block. The sensor also utilizes in house designs of a Wilkinson Power Divider (WPD), single-balanced diode mixer in a six-port configuration and three-element series fed patch antenna for both transmit and receive. The most critical component of the radar front end is an in house designed P-I-N diode reflection-based quadrature phase shifter to facilitate the digital phase modulation required for PMCW radar.

The respective components used on the board are the Analog Devices HMC739 VCO, the Mini-Circuits PMA3-15453+ gain block, and Qorvo CMD298C4 LNA. The P-I-N diodes used in the reflection phase shifter are the MACOM MADP-000907-14020 that feature a 2ns switching time and are operational up to 70 GHz. For the single balanced diode mixer, the Infineon BAT-24 -02LS low barrier Schottky diodes are utilized. The down-converted signal is then sent to a baseband board designed on FR4 substrate.

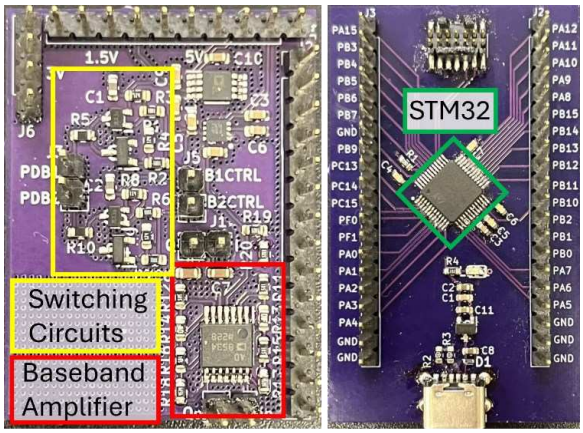

(a) (b)

Fig. 4. (a) Baseband board with AD8534 operational amplifier and switching circuits (b) STM32G473CET6 breakout board for control signals.

B. Baseband Hardware

Fig. 4 (a) shows the baseband FR4 board used to amplify the low frequency voltage signal at the output of the radar front end. An AC coupled baseband amplifier was designed using an Analog Devices AD8534 operational amplifier IC. The amplifier features two stages of voltage gain in an inverting amplifier configuration. The amplifier provides 10 times amplification in the first stage and 4.5 times in the second stage for a total of 33 dB of voltage gain. The output I and Q signals are measured by an oscilloscope and saved to a .csv file for MATLAB processing.

The baseband board also includes a MOSFET based switching circuit that provides the necessary bias voltage and forward current to activate the P-I-N diodes. This circuit features the Infineon BSS209-PW-DS PMOS and Infineon BSS119-DS NMOS because of the favorable PMOS IV curve and because both transistors operate with 3.3V logic. The resistors in the circuit are optimized for proper operation of the switching circuit and to limit the output current of the circuit so the P-I-N diodes are properly activated but consume the minimum amount of DC power. The bias resistors at the input of the circuit are also used to limit the current sourced from the microcontroller that is providing the control signal to the switching circuit. Limiting current sourced from the microcontroller is important to avoid damaging the sensitive electronics in the chip.

The second baseband board on FR4 substrate is shown in Fig. 4 (b). This board is a simple breakout board designed for the ST Microelectronics STM32G473CET6 microcontroller. The STM32 generates the PRBS that controls the switching circuit and therefore the P-I-N diode phase shifter and PMCW phase modulation. The µC is programmed through the 14-pin header shown at the top of Fig. 4 (b) and the accessible GPIO pins lead to the pin headers lining the outside of the board.

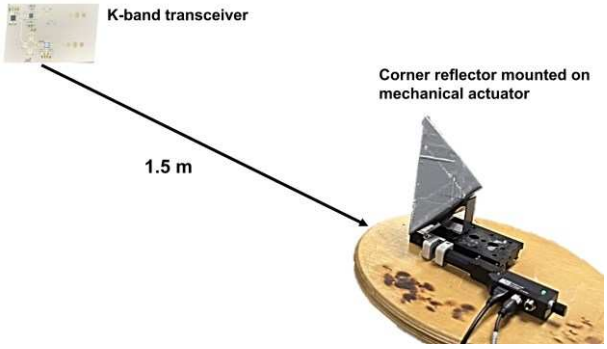

Fig. 5. PMCW Radar experimental setup with 24 GHz transceiver and corner reflector on a mechanical actuator for accurate small motions

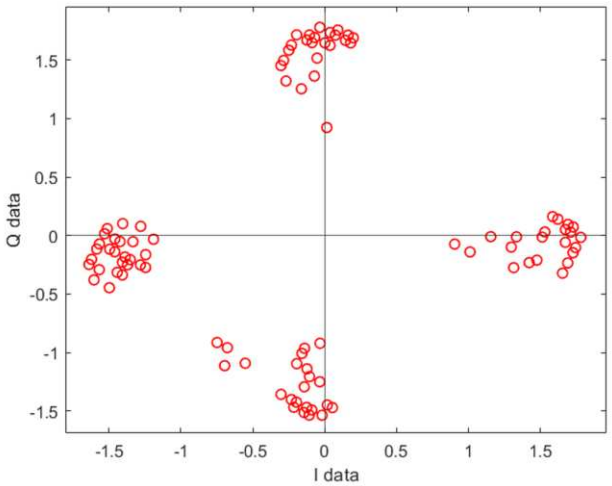

Fig. 6. Corrected QPSK PMCW *I/Q* constellation diagram collected from presented *K*-Band front end radar sensor

IV. Experimental Results

A. Experimental Setup

To test the QPSK PMCW radar architecture a corner reflector mounted on a mechanical actuator was placed approximately 1.5 meters from the sensor. Fig. 5 gives a visual example of the experimental setup. The data from the radar system was recorded using an oscilloscope and further processed using MATLAB. The actuator was programmed to move a total of 1mm peak to peak at a frequency of 5 Hz.

B. Results

Fig. 6 shows the corrected *I/Q* constellation from the output of the radar. During the MATLAB processing stage, the *I/Q* channel imbalance and arbitrary phase modulation was corrected using a PMCW correction algorithm.

It can be seen from Fig. 6 that the experimental radar data creates an *I/Q* constellation with four distinct points corresponding to the four phase states of QPSK. Due to limitations in the high frequency bit stream encoding and sampling rates, range detection was not carried out and is a topic of future work. However, it can be inferred from the experimental results and simulation that the radar would be able to effectively detect range with acceptable range resolution when proper symbol and sampling rates are used.

V. Conclusion

A *K*-Band QPSK PMCW radar with digital *I/Q* constellation phase compensation and *I/Q* imbalance correction was constructed, simulated and presented for future PMCW radar systems. Future works from the author will include analysis of the challenges and considerations related to the implementation of a QPSK PMCW radar. Future works will also focus on improvement of the designed *K*-Band front end to allow for higher speed phase encoding and full experimental verification of the range detection and benefits of QPSK PMCW radar over common BPSK based systems.

References

[1] M. Brown and C. Li, “Advancement of PMCW Radar and Its Board-Level Prototyping,” in *2023 IEEE 16th Dallas Circuits and Systems Conference (DCAS)*, Apr. 2023, pp. 1–4. doi: 10.1109/DCAS57389.2023.10130242.

[2] M. Umehira *et al.*, “Inter-radar interference in automotive FMCW radars and its mitigation challenges,” in *2020 IEEE International Symposium on Radio-Frequency Integration Technology (RFIT)*, Sep. 2020, pp. 220–222.

[3] S. Alland, W. Stark, M. Ali and M. Hegde, "Interference in Automotive Radar Systems: Characteristics, Mitigation Techniques, and Current and Future Research," in *IEEE Signal Processing Magazine*, vol. 36, no. 5, pp. 45-59, Sept. 2019, doi: 10.1109/MSP.2019.2908214.

[4] R. Lin, Z. Liu, Y. Chen, H. C. So and J. Li, "Theoretical Insights and Practical Algorithms for Transceiver Design of PMCW Radar," in *IEEE Transactions on Signal Processing*, vol. 72, pp. 3091-3103, 2024, doi: 10.1109/TSP.2024.3409614.

[5] H. Griffiths, "Where has all the spectrum gone?" 2013 International Conference on Radar, Adelaide, SA, Australia, 2013, pp. 1-5

[6] D. Guermandi *et al*., "A 79-GHz 2 × 2 MIMO PMCW Radar SoC in 28-nm CMOS," in *IEEE Journal of Solid-State Circuits*, vol. 52, no. 10, pp. 2613-2626, Oct. 2017, doi: 10.1109/JSSC.2017.2723499.

[7] F. Probst, A. Engelmann, P. Hetterle, V. Issakov, R. Weigel, and M. Dietz, “A 15-Gb/s PMCW Radar PRBS-Generator for MIMO and Joint Radar-Communication Systems,” in *2022 Asia-Pacific Microwave Conference (APMC)*, Nov. 2022, pp. 288–290. doi: 10.23919/APMC55665.2022.9999774.

[8] “Sensors | Free Full-Text | Doppler Shift Tolerance of Typical Pseudorandom Binary Sequences in PMCW Radar”, Accessed: Jul. 22, 2024. [Online]. Available: https://www.mdpi.com/1424-8220/22/9/3212

[9] M. M. Madankar and P. S. Ashtankar, “Performance analysis of BPSK modulation scheme for different channel conditions,” in *2016 IEEE Students’ Conference on Electrical, Electronics and Computer Science (SCEECS)*, Mar. 2016, pp. 1–5. doi: 10.1109/SCEECS.2016.7509290.

[10] M. A. N. Chowdhury, M. R. Ullah Mahfuz, S. H. Chowdhury, and Md. M. Kabir, “Design of an improved QPSK modulation technique in wireless communication systems,” in *2017 3rd International Conference on Electrical Information and Communication Technology (EICT)*, Dec. 2017, pp. 1–6. doi: 10.1109/EICT.2017.8275196.

[11] A. D. Droitcour, O. Boric-Lubecke, V. M. Lubecke, J. Lin, and G. T. A. Kovacs, “Range correlation and I/Q performance benefits in single-chip silicon Doppler radars for noncontact cardiopulmonary monitoring,” *IEEE Transactions on Microwave Theory and Techniques*, vol. 52, no. 3, pp. 838–848, Mar. 2004, doi: 10.1109/TMTT.2004